ORIGINAL ARTICLE:

Effective sequestration of *Clostridium difficile* protein toxins by calcium aluminosilicate

RUNNING TITLE: *Clostridium difficile* toxin sequestration

Joseph M. Sturino[a,#], Karina Pokusaeva[a] and Robert Carpenter[b,c]

[a] Nutrition and Food Science Department, Texas A&M University,
College Station, Texas 77843

[b] Texas EnteroSorbents, Inc., Bastrop, Texas 78602

[c] Salient Pharmaceuticals Incorporated, Houston, Texas 77005

[#] **Corresponding Author:** Dr. Joseph M. Sturino;
Telephone: +1 (805) 317-4243; E-Mail: joseph.sturino@gmail.com;
URL: www.josephsturino.com/

ABSTRACT:

Clostridium difficile is a leading cause of antibiotic-associated diarrhea and the etiologic agent responsible for *C. difficile* infection. TcdA and TcdB are nearly indispensible virulence factors for *Clostridium difficile* pathogenesis. Given the toxin-centric mechanism by which *C. difficile* pathogenesis occurs, the selective sequestration and neutralization of TcdA and TcdB by non-antibiotic agents represents a novel mode of action to prevent or treat *C. difficile*-associated disease. In this preclinical study, we used quantitative enzyme immunoassays to determine the extent by which a novel drug, calcium aluminosilicate uniform particle size Novasil (CAS UPSN M-1), is capable of sequestering TcdA and TcdB *in vitro*. The following major findings were derived from the present study: Firstly, CAS UPSN M-1 efficiently sequestered both TcdA and TcdB to undetectable levels. Secondly, we show that CAS UPSN M-1's affinity for TcdA is greater than its affinity for TcdB. Lastly, we show that CAS UPSN M-1 exhibited limited binding affinity for non-target therapeutic proteins. Together, these results suggest that ingestion of calcium aluminosilicate might protect gastrointestinal tissues from antibiotic- or chemotherapy-induced *C. difficile* infection by neutralizing the cytotoxic and pro-inflammatory effects of luminal TcdA and TcdB.

KEYWORDS: *Clostridium difficile*, TcdA, TcdB, calcium aluminosilicate, gastrointestinal inflammation, quantitative enzyme immunoassay

INTRODUCTION

Clostridium difficile is a leading cause of antibiotic-associated diarrhea (AAD) and the etiologic agent responsible for *C. difficile*-associated infection (CDI). CDI typically starts as a mild diarrhea but rapidly degenerates into a variety of potentially life-threatening conditions, including sepsis syndrome and pseudomembranous colitis (1). In the United States, approximately 330,000 cases of CDI are estimated each year (2); however the incidence of *C. difficile* infection continues to increase (2-3). Increasing CDI rates highlight that current infection control procedures and treatment options are insufficient.

In the healthcare setting, endospore-forming *C. difficile* are transmitted to patients via the fecal-oral route (4). Following exposure, the host's gastrointestinal microbiota typically either quells a nascent *C. difficile* infection or suppresses it to sub-clinical levels (5). As a result of the latter, approximately 20% of hospitalized adults become asymptomatic *C. difficile* carriers, while carriage rates approach 50% for patients in long-term care (6-9). The likelihood of developing CDI increases in patients with dysbiotic gastrointestinal microbiota, since *C. difficile* can thrive in the dysbiotic niche (5, 10). This dysbiosis is often the result of non-specific chemotherapies that are used to treat conditions unrelated to *C. difficile* infection (*e.g.*, antibacterial agents or antineoplastic drugs).

The antibiotics metronidazole and vancomycin are currently used to treat CDI (11). Unfortunately, given the conflicting roles of antibiotics in the establishment and resolution of CDI, *C. difficile* AAD is recurrent in up to 1 in 5 patients (12). These already high reoccurrence rates are expected to increase if *C. difficile* strains with

intermediate- and complete-resistance to metronidazole and vancomycin emerge (13). Together, these alarming trends illustrate an urgent need to develop novel and efficacious therapeutics to treat CDI, including non-traditional therapeutic agents.

C. difficile is an extracellular pathogen and it typically does not invade host tissues. While a number of *C. difficile*-encoded virulence factors are responsible for *C. difficile* carriage and pathogenesis, toxin A (TcdA) and toxin B (TcdB) are among the best-studied (14). Once secreted into the colon, these cytotoxic protein-based enzymes are translocated across the membrane bilayer and into the cytosol by receptor-mediated endocytosis (15). Once inside the cell, these glycosyltransferases trigger altered cellular transcription, which results in significant cellular apoptosis and tissue remodeling (16-18). TcdA and TcdB are also strongly pro-inflammatory, which exacerbates their effects on structural and functional changes in tissue integrity (19-20). Together, these inflammation-related activities contribute to the progressive ablation of gastrointestinal function that is characteristic of CDI. In animal models, the administration of purified *C. difficile* TcdA induces the hallmark symptoms of an acute, pseudomembranous colitis-like condition: edema, gastrointestinal inflammation, cellular necrosis, and gastroenteritis in the absence of the bacterium (19, 21-23). The administration of TcdB elicits similar effects, albeit to a lesser degree (22, 24). As a result, these protein-based enzymes have been ascribed as nearly indispensible determinants for *C. difficile* pathogenesis.

Given the toxin-centric mechanism by which *C. difficile* pathogenesis occurs, the selective sequestration and neutralization of TcdA and TcdB by non-antibiotic agents represents a novel mode of action to prevent or treat *C. difficile*-associated diseases (25-26). To date, four *C. difficile* toxin-binding agents have been examined in pre-clinical

studies: cholestyramine, colestipol, synsorb 90, and tolevamer (25). Of these toxin-binding agents, only three have been tested in clinical studies. Unfortunately, none of these agents have proven to be as efficacious as traditional antibiotic therapies. Nevertheless, it is important to continue to develop new candidate therapies. In this manuscript, we describe the characterization of CAS UPSN M-1, a novel calcium aluminosilicate agent that has been developed to selectively bind to and neutralize large clostridial protein toxins. Calcium aluminosilicate is recognized by the Food and Drug Administration (FDA) as a Generally Regarded as Safe (GRAS) additive, which can be supplemented to foods at levels up to 2% (w/w) (27).

MATERIALS AND METHODS

Protein-based cytotoxic enzymes and reagents. Lyophilized *C. difficile* TcdA and *C. difficile* TcdB were stored according to the manufacturer's specification (Calbiochem, Gibbstown, NJ). TcdA and TcdB were resuspended in 10 mM 2,2-bis(hydroxymethyl)-2,2′,2-nitrilotriethanol (Bis-Tris) buffer (Sigma-Aldrich, St. Louis, MO) and maintained on ice prior to being assayed. All other chemicals were molecular biology grade and stored as recommended by the manufacturer. A SevenMulti conductivity meter (Mettler Toledo, Columbus, OH) was used for pH measurements.

Putative toxin binding agent. Calcium aluminosilicate uniform particle size Novasil M-1 (CAS UPSN M-1), the novel sequestering agent used in this study, was provided by Salient Pharmaceuticals Incorporated (Houston, TX).

Quantitative enzyme immunoassay (qEIA) for toxin quantification. The concentration of *C. difficile* TcdA or TcdB was measured using the Premier Toxins A&B

enzyme immunoassay (EIA) according to the manufacture's instructions (Meridian Bioscience Inc., Cincinnati, OH) except that a series of assay positive control samples (*i.e.*, TcdA and TcdB reference standards at a range of known concentrations) was incorporated into each repeated measurement; the concentration of these reference standards typically ranged from 5 to 20 ng/ml. In brief, the resultant qEIA uses *C. difficile* TcdA- and TcdB-specific polyclonal antibodies to capture TcdA and TcdB and to non-covalently anchor them to the solid-phase EIA support matrix. Matrix-bound toxins were subsequently complexed with horseradish peroxidase (HRP)-conjugated mouse anti-toxin A (monoclonal) or goat anti-toxin B (polyclonal) antibodies, respectively. After the removal of unbound HRP-antibody conjugates, degradation of urea hydrogen peroxide by toxin-bound horseradish peroxidase was assayed in the presence of the reducing co-substrate 3,3′,5,5′-tetramethyl-[1,1′-biphenyl]-4,4′-diamine (TMB). Phosphoric acid (1 M) was used to arrest the reaction. The terminal chromophore benzidine-4,4′-diimine (BZDI), an oxidized derivative of TMB, was measured in arbitrary units (AU) at an optical density of 450 nm ($OD_{450\ nm}$) using an Infinite M200 microplate reader (Tecan US Inc., Durham, NC). The Infinite M200 iControl software was used to generate custom EIA microplate templates to speed data acquisition and to ensure accurate sample assignation.

Toxin sequestration assays. This qEIA was used to assess the sequestration (an aggregate of adsorption and absorption) of large clostridial protein toxins by calcium aluminosilicate. Unless otherwise indicated, calcium aluminosilicate was suspended up to a final concentration of 0.5 mg/ml in 10 mM Bis-Tris (pH 6.5) and pre-equilibrated to 37°C in a Thermomixer R shaking incubator (Eppendorf, Hauppauge, NY) equipped with

a 1.5-ml block with constant agitation at 1,200 revolutions per minute (rpm). Individual sequestration reactions were started by the addition of the toxin to a final concentration of 10 ng/ml (TcdA) or 15 ng/ml (TcdB), unless otherwise indicated. Sequestration reactions were then incubated for 10 min at 37°C with constant agitation at 1,200 rpm in a Thermomixer R (Eppendorf). The sequestration reaction was stopped when the residual calcium aluminosilicate and calcium aluminosilicate-bound toxin complexes were pelleted by centrifugation (2 min at 21,130 × *g*) in a 5424 bench top centrifuge (Eppendorf). Following centrifugation, the clarified supernatant was carefully removed by aspiration, transferred to a 1.5 ml tube, and chilled on ice prior to toxin quantification using the qEIA described above.

Heterologous, non-therapeutic protein-binding and SDS-PAGE. Calcium aluminosilicate (5 mg/ml) was co-incubated with the SeeBlue Plus2 protein ladder (750 µg/ml; Invitrogen, San Diego, CA), which contains a number of non-therapeutic target proteins. Samples were incubated at 37°C for 20 min with constant agitation (1,200 rpm). The reaction was stopped when the residual calcium aluminosilicate and calcium aluminosilicate-bound protein complexes were pelleted by centrifugation (2 min at 21,130 × *g*) in an Eppendorf 5424 bench top centrifuge (Eppendorf). The supernatant was carefully transferred to a fresh tube and set on ice. The pellet containing the residual calcium aluminosilicate and calcium aluminosilicate-bound protein complexes was re-suspended in 1 volume buffer and agitated for 20 min at (1,200 rpm). The unbound calcium aluminosilicate and calcium aluminosilicate-bound protein complexes were again pelleted by centrifugation (2 min at 21,130 × *g*). The resultant pellet eluate—including any proteins eluted from the calcium aluminosilicate—was carefully transferred

to a fresh tube. Negative control samples (*i.e.*, SeeBlue Plus2 devoid of calcium aluminosilicate) were otherwise treated identically to experimental samples.

The original supernatant and the pellet eluate were both subjected to polyacrylamide gel electrophoresis (PAGE). Samples (15 µl) were loaded into the 1-mm wells of a NuPAGE Novex Tris-Acetate gel (Invitrogen) using 1× lithium dodecyl sulfate (LDS) sample buffer (Invitrogen). Protein electrophoresis was carried out (150 V for 1 h) in an Xcell SureLock Mini Cell (Invitrogen) and 1× NuPAGE tris-acetate SDS running buffer (Invitrogen). Proteins were stained using the SimplyBlue Safe Stain (Invitrogen) according to the manufacturer's instruction. The results were captured using the FluorChem HD2 documentation system with a 5 MHz cooled digital CCD camera (Alpha Innotech).

Biostatistics. Raw qEIA data were captured using the Infinite M200 i-Control software, exported to Excel (Microsoft Corporation, Redmond, WA), and analyzed using Prism (GraphPad Software Inc., La Jolla, CA). Unless otherwise indicated, data represent at least three repeated measures. Data are expressed as the mean ($\bar{x}$) ± either the standard error of the mean (SEM) or standard deviation (SD), as noted. Calibration curves were generated by least-squares regression. ANOVA was used to determine the statistical significance of the measured differences between treatments. When significant differences were detected by ANOVA, Bonferroni tests were performed *posthoc* in order explore these differences. An associated p value of less than 0.05 was considered statistically significant. The base-10 logarithm (log_{10}) of each data point was calculated and a calibration curve for the interpolation of unknowns was generated using least-squares linear regression.

RESULTS

Optimization of a quantitative enzyme immunoassay (qEIA) to detect TcdA and TcdB. Samples containing known concentrations of TcdA or TcdB were used to generate standard curves. The standard curves from each of six randomly selected vials of TcdB are plotted in **FIGURE 1.** A one-factor ANOVA found toxin vial-specific effects were statistically significant ($p < 0.0051$); however, *posthoc* comparisons using the Bonferroni test indicated that—with the exception of one obvious outlier ($p < 0.05$)—differences between the remaining five curves were statistically nonsignificant ($p > 0.05$). For this experimental subset ($n = 5$), the Pearson product-moment correlation coefficient (r) indicated a strong, co-linear relationship between toxin concentration and optical density that was statistically significant between inter-experimental EIA replicates ($r = 0.9078$, $p = 0.0047$). Similar results were seen for TcdA ($n = 5$), although differences between individual vials of TcdA were statistically nonsignificant ($p = 0.8707$). As seen with TcdB, a strong co-linear relationship between toxin concentration and optical density was observed. This co-linear relationship was statistically significant between inter-experimental qEIA replicates ($r = 0.9973$, $p = 0.0027$). In separate experiments that examined the effect of toxin thermostability, differences in qEIA reactivity following short-term (*e.g.*, 8 h) incubation on ice were found to be statistically nonsignificant ($p > 0.05$). As a result, individual toxin vials were used to conduct multiple sequestration assays within a single workday and were then discarded.

Data distribution and transformation. The descriptive statistic skewness (g_1) and the Kolmogorov-Smirnov (K-S) normality test were used to examine the data distribution within the TcdA and TcdB datasets. While both datasets skewed right

(TcdA: $g_1 = 0.6626$; TcdB: $g_1 = 1.331$), the K-S test indicated that neither exhibited significant differences from the Gaussian distribution ($p > 0.10$). Nevertheless, the base-10 logarithm (log_{10}) of each datapoint was calculated to normalize the data. Linear regressions of mean TcdA ($n = 4$; $R^2 = 0.968$) and TcdB ($n = 5$; $R^2 = 0.966$) reference curves are plotted in **FIGURE 2.** Signal response plateaus were observed at very high toxin concentrations and very low toxin concentrations (data not shown).

Calcium aluminosilicate does not affect the pH of the qEIA. In order to determine if calcium aluminosilicate might artificially diminish the sensitivity of the qEIA by affecting the pH of the buffer system, calcium aluminosilicate was supplemented to a final working concentration of 0.5 mg/ml in 100 mM Tris (pH 6.5) and the pH was measured ($n = 3$) once the mixture was equilibrated to 37°C. Incorporation of calcium aluminosilicate up to 0.5 mg/ml did not affect the pH of the buffer system ($\bar{x} =$ 6.52, SD = 0.01) when compared to a buffer control that was devoid of calcium aluminosilicate ($\bar{x} = 6.50$, SD = 0.001), as expected.

Effective, dose-dependent sequestration of large *C. difficile* cytotoxic enzymes by calcium aluminosilicate. Calcium aluminosilicate was assessed for its ability to reduce the concentration of large clostridial protein-based cytotoxic enzymes *in vitro.* During these dose-response experiments, the concentration of TcdA or TcdB (**FIGURE 3**) was fixed at 10 ng/ml, while the calcium aluminosilicate concentration was varied 100-fold (*i.e.*, 0.05 mg/ml, 0.075 mg/ml, 0.1 mg/ml, 0.3 mg/ml, 0.5 mg/ml, 0.75 mg/ml, 1 mg/ml, 2 mg/ml, 3 mg/ml, and 5 mg/ml). Calcium aluminosilicate efficiently sequestered TcdA and TcdB *in vitro*. Differences in mean endpoint $OD_{450\ nm}$ between the assay negative control (*i.e.,* vehicle devoid of TcdA) samples ($\bar{x} = 0.044$ AU, SD = 0.001 AU)

and experimental samples supplemented with calcium aluminosilicate up to 2 mg/ml ($\bar{x}$ = 0.049 AU, SD = 0.004 AU), 3 mg/ml ($\bar{x}$ = 0.049 AU, SD = 0.005 AU), and 5 mg/ml ($\bar{x}$ = 0.048 AU, SD = 0.004 AU) were statistically nonsignificant ($p > 0.05$).

The raw qEIA measurements obtained from experimental samples were converted to residual toxin concentrations using intra-experimental EIA calibration curves. Differences in residual TcdA concentration between the assay positive control (*i.e.*, TcdA-containing samples devoid of calcium aluminosilicate) samples and experimental samples containing calcium aluminosilicate supplemented up to 0.05 mg/ml ($\bar{x}$ = 11.11 ng/ml, SD = 1.82 ng/ml), 0.075 mg/ml ($\bar{x}$ = 11.35 ng/ml, SD = 0.22 ng/ml), and 0.1 mg/ml ($\bar{x}$ = 10.93 ng/ml, SD = 0.06 ng/ml) were statistically nonsignificant (**FIGURE 3**). In contrast, statistically significant differences in residual TcdA concentrations were measured between the assay positive control and experimental samples containing calcium aluminosilicate supplemented to 0.3 mg/ml ($\bar{x}$ = 8.54 ng/ml, SD = 1.19 ng/ml, $p < 0.05$), 0.5 mg/ml ($\bar{x}$ = 4.88 ng/ml, SD = 0.80 ng/ml, $p < 0.001$), 0.75 mg/ml ($\bar{x}$ = 3.20 ng/ml, SD = 0.65 ng/ml, $p < 0.001$), 1 mg/ml ($\bar{x}$ = 1.67 ng/ml, SD = 0.71 ng/ml), 2 mg/ml ($\bar{x}$ = below the lower limit of detection (bLLD), $p < 0.001$), 3 mg/ml ($\bar{x}$ = bLLD, $p < 0.001$), and 5 mg/ml ($\bar{x}$ = bLLD, $p < 0.001$). The lower limit of detection for this qEIA is approximately 1.4 ng/ml for TcdA and 2.4 ng/ml for TcdB.

The efficiency by which the calcium aluminosilicate calcium aluminosilicate sequestered TcdB was also explored (**FIGURE 3**). Differences in endpoint $OD_{450\ nm}$ measurements between the assay negative control (*i.e.,* vehicle devoid of TcdB) samples ($\bar{x}$ = 0.047 AU, SD = 0.004 AU) and experimental samples supplemented with calcium aluminosilicate up to 3 mg/ml ($\bar{x}$ = 0.043 AU, SD = 0.001 AU), and 5 mg/ml ($\bar{x}$ = 0.041

AU, SD = 0.002 AU) were statistically nonsignificant ($p > 0.05$). As performed with TcdA, the raw qEIA measurements were converted to residual toxin concentrations. Differences in residual TcdB concentration between the assay positive control (*i.e.*, TcdB-containing samples devoid of calcium aluminosilicate) samples and experimental samples containing calcium aluminosilicate supplemented up to 0.05 mg/ml ($\bar{x}$ = 9.07 ng/ml, SD = 0.06 ng/ml), 0.075 mg/ml ($\bar{x}$ = 8.75 ng/ml, SD = 0.05 ng/ml), 0.1 mg/ml ($\bar{x}$ = 9.02 ng/ml, SD = 1.38 ng/ml), and 0.3 mg/ml ($\bar{x}$ = 8.44 ng/ml, SD = 0.8 ng/ml) were statistically nonsignificant ($p > 0.05$). In contrast, statistically significant differences in residual TcdB concentrations were measured between the assay positive control and experimental samples containing calcium aluminosilicate supplemented up to 0.5 mg/ml ($\bar{x}$ = 6.27 ng/ml, SD = 0.36 ng/ml, $P < 0.001$), 0.75 mg/ml ($\bar{x}$ = 5.47 ng/ml, SD = 0.64 ng/ml; $p < 0.001$), 1 mg/ml ($\bar{x}$ = 4.99 ng/ml, SD = 1.23 ng/ml), 2 mg/ml ($\bar{x}$ = 3.75 ng/ml; $p < 0.001$), 3 mg/ml ($\bar{x}$ = bLLD, $p < 0.001$), and 5 mg/ml ($\bar{x}$ = bLLD, $p < 0.001$).

The protein-binding activity of calcium aluminosilicate. The selectivity of calcium aluminosilicate's protein-binding activity was explored further using a variation of the *C. difficile* toxin-binding assay described above. During these experiments, calcium aluminosilicate (5 mg/ml) was challenged with a commercial protein cocktail that contained a number of non-therapeutic proteins, including myosin, bovine serum albumin, and glutamate dehydrogenase. A representative SDS-PAGE gel of the supernatant and the pellet eluate can be found in **FIGURE 4**. CAS UPSN M-1 bound non-therapeutic proteins, but did so with varying efficiency. Indeed, CAS UPSN M-1 bound myosin and bovine serum albumin inefficiently, while glutamate dehydrogenase was bound efficiently. Attempts to elute proteins bound to CAS UPSN M-1 were

unsuccessful (**FIGURE 4**, lanes 4-5), which suggests that proteins bound to CAS UPSN M-1 are bound tightly.

DISCUSSION

The initial toxin concentrations used in this study were selected because they approximated the median concentration of TcdA (4.3 ng/ml) that is typically found in the stool of patients with *C. difficile*-associated diarrhea (range 0.6 ng/ml to 19 µg/ml) (28). As such, the developed qEIA protocol enabled *C. difficile* TcdA and TcdB quantification at clinically relevant concentrations. No hook effect was obvious for either toxin at toxin concentrations between 5 to 15 ng/ml, which constituted the linear range for this qEIA. The high-dose hook effect occurs when the antigen negatively affects the binding capacity of the reporter antibody or when it is added in excess of the reporter antibody (29). The intra-experimental EIA calibration curves generated using this qEIA protocol enabled toxin quantification via interpolation and, thus, facilitated the conversion of optical density measurements to residual toxin concentrations. Furthermore, given the high degree of reproducibility, this qEIA supported inter-experimental comparisons between repeated measurements (*e.g.*, randomized block experiments).

This assay revealed that calcium aluminosilicate efficiently removed both TcdA and TcdB at physiologically relevant concentrations. Indeed, calcium aluminosilicate neutralized TcdA to sub-clinical levels *in vitro*. Like tolevamer, protein binding by calcium aluminosilicate does not occur in a generalized or otherwise indiscriminate fashion and, thus, displays a degree of target specificity. Tolevamer is an anionic, high-molecular-weight polymer (>400 kDa) that was developed to neutralize TcdA and TcdB.

Tolevamer has been shown to ameliorate CDI-like symptoms in hamsters (30). In addition, tolevamer has demonstrated therapeutic efficacy in a number of phase II and phase III clinical studies (25-26). While effective, tolevamer's cure rate was found to be inferior to those of vancomycin and metronidazole (26, 31). Surprisingly, however, the rate of CDI reoccurrence was generally lower with tolevamer than with either vancomycin or metronidazole (26)

TcdA and TcdB are postulated to be paralogs (32-33). As a result, these proteins share significant amino acid sequence similarity to one another—especially at their amino- and carboxy-terminal regions. Both toxins share approximately 47% identity to each other and approximately 68% sequence similarity (data not shown). Both proteins are comprised of three well-characterized functional domains (15). The amino-terminus of the protein encodes a peptidase C80-type glycosyltransferase domain and a proximal substrate recognition domain. The hydrophobic middle region is putatively involved in membrane translocation. The carboxy terminus of the protein encodes the clostridial repetitive oligopeptides (CROPS)—also known as cell wall binding (CWB) domains. The carboxy-terminal CROPS facilitate calcium-dependent host cell recognition (33), and may also play a role in the sequestration of TcdA and TcdB by calcium aluminosilicate. Proteins that are evolutionarily and/or structurally related to TcdA and TcdB might also be viable therapeutic targets for calcium aluminosilicate, however additional research is required to test this hypothesis.

In addition to the similarities noted above, a number of toxin-specific differences were also observed. For example, the lowest experimental concentration of calcium aluminosilicate for which there was no observable effect was 0.1 mg/ml for TcdA, but 0.3

mg/ml for TcdB. The minimum effective concentration (*i.e.*, the threshold dose) for calcium aluminosilicate was 0.3 mg/ml for TcdA, but 0.5 mg/ml for TcdB. Under these conditions, the calcium aluminosilicate concentration that achieved maximum efficacy (EC_{100}) was 2 mg/ml for TcdA, but the concentration of calcium aluminosilicate that provided approximately 50% of the maximum effect (EC_{50}) for TcdA was 0.5 mg/ml. In contrast the EC_{100} and EC_{50} for TcdB were 3 mg/ml and 1 mg/ml, respectively. While calcium aluminosilicate sequesters both protein-based cytotoxic enzymes, these results suggest that its affinity for TcdA is greater than its affinity for TcdB.

As antibiotic resistant pathogens continue to emerge, the development of non-antibiotic treatment options represents a timely therapeutic approach to CDI management. Calcium aluminosilicate exhibited potent *C. difficile* TcdA- and TcdB-neutralizing activity and selective protein binding *in vitro*. Given the well-documented safety profile of calcium aluminosilicate (34), these studies provide *in vitro* evidentiary support our hypothesis that ingestion of calcium aluminosilicate might protect gastrointestinal tissues and accelerate a patient's recovery from antibiotic- or chemotherapy-induced, *C. difficile*-associated diarrhea by neutralizing the cytotoxic effects of luminal TcdA and TcdB. Depending on its relative effectiveness and tolerability during downstream clinical studies, CAS UPSN M-1, the novel sequestration agent described in this study, may be used to complement or, possibly, replace existing antibiotic therapies for the treatment of CDI. However, it is beyond the scope of this current study to examine the biological effects of calcium aluminosilicate *in vivo*.

ACKNOWLEDGEMENTS

Salient Pharmaceuticals Incorporated (Houston, TX) provided the calcium aluminosilicate (CAS UPSN M-1) used in this study without cost. Salient Pharmaceuticals, LLC (Houston, TX) provided funding for this study to Texas A&M AgriLife Research (JMS). Additional support was provided by the United States Department of Agriculture, Cooperative State Research, Education and Extension Service Hatch project TEX 09436 and Texas A&M AgriLife Research. The sponsors had no role in the data collection or analysis, the production of the submitted manuscript, or the decision to submit the manuscript for publication.

The authors would like to thank Trung Nguyen and Lynn Jones for technical support. In addition, the authors would like to thank Richard Scruggs at Salient Pharmaceuticals Incorporated for insightful conversations and Michael Pendleton at the Microscopy and Imaging Center at Texas A&M University (College Station, Texas, USA) for assistance with scanning electron microscopy. Lastly, the authors would like to thank the anonymous reviewers for their valuable comments.

REFERENCES

1. **Eaton SR, Mazuski JE.** 2013. Overview of severe *Clostridium difficile* infection. Crit. Care Clin. **29:**827-839.
2. **Lessa FC, Gould CV, McDonald LC.** 2012. Current status of *Clostridium difficile* infection epidemiology. Clin. Infect. Dis. **55**(Suppl 2)**:**S65-70.
3. **Gerding DN.** 2010. Global epidemiology of *Clostridium difficile* infection in 2010. Infect. Control Hosp. Epidemiol. **31**(Suppl 1)**:**S32-34.
4. **Sunenshine RH, McDonald LC.** 2006. *Clostridium difficile*-associated disease: new challenges from an established pathogen. Cleve. Clin. J. Med. **73:**187-197.
5. **Britton RA, Young VB.** 2014. Role of the intestinal microbiota in resistance to colonization by *Clostridium difficile*. Gastroenterology. **146:**1547-1553.
6. **Riggs MM, Sethi AK, Zabarsky TF, Eckstein EC, Jump RL, Donskey CJ.** 2007. Asymptomatic carriers are a potential source for transmission of epidemic and nonepidemic *Clostridium difficile* strains among long-term care facility residents. Clin. Infect. Dis. **45:**992-998.
7. **Ryan J, Murphy C, Twomey C, Paul Ross R, Rea MC, MacSharry J, Sheil B, Shanahan F.** 2010. Asymptomatic carriage of *Clostridium difficile* in an Irish continuing care institution for the elderly: prevalence and characteristics. Ir. J. Med. Sci. **179:**245-250.
8. **Rea MC, O'Sullivan O, Shanahan F, O'Toole PW, Stanton C, Ross RP, Hill C.** 2012. *Clostridium difficile* carriage in elderly subjects and associated changes in the intestinal microbiota. J. Clin. Microbiol. **50:**867-875.
9. **Hung YP, Lee JC, Lin HJ, Liu HC, Wu YH, Tsai PJ, Ko WC.** 2014. Clinical impact of *Clostridium difficile* colonization. J. Microbiol. Immunol. Infect.
10. **Pérez-Cobas AE, Artacho A, Ott SJ, Moya A, Gosalbes MJ, Latorre A.** 2014. Structural and functional changes in the gut microbiota associated to *Clostridium difficile* infection. Front. Microbiol. **5:**335.
11. **Luciano JA, Zuckerbraun BS.** 2014. *Clostridium difficile* infection: prevention, treatment, and surgical management. Surg. Clin. North Am. **94:**1335-1349.
12. **Fekety R, McFarland LV, Surawicz CM, Greenberg RN, Elmer GW, Mulligan ME.** 1997. Recurrent *Clostridium difficile* diarrhea: characteristics of and risk factors for patients enrolled in a prospective, randomized, double-blinded trial. Clin. Infect. Dis. **24:**324-333.
13. **Shah D, Dang MD, Hasbun R, Koo HL, Jiang ZD, DuPont HL, Garey KW.** 2010. *Clostridium difficile* infection: update on emerging antibiotic treatment options and antibiotic resistance. Expert Rev. Anti. Infect. Ther. **8:**555-564.
14. **Awad MM, Johanesen PA, Carter GP, Rose E, Lyras D.** 2014. *Clostridium difficile* virulence factors: insights into an anaerobic spore-forming pathogen. Gut Microbes. 1:0.
15. **Voth DE, Ballard JD.** 2005. *Clostridium difficile* toxins: mechanism of action and role in disease. Clin. Microbiol. Rev.**18:**247-263.
16. **Just I, Gerhard R.** 2004. Large clostridial cytotoxins. Rev. Physiol. Biochem. Pharmacol. **152:**23-47.

17. **Feltis BA, Wiesner SM, Kim AS, Erlandsen SL, Lyerly DL, Wilkins TD, Wells CL.** 2000. *Clostridium difficile* toxins A and B can alter epithelial permeability and promote bacterial paracellular migration through HT-29 enterocytes. Shock. **14:**629-634.
18. **Farrow MA, Chumbler NM, Lapierre LA, Franklin JL, Rutherford SA, Goldenring JR, Lacy DB.** 2013. *Clostridium difficile* toxin B-induced necrosis is mediated by the host epithelial cell NADPH oxidase complex. Proc. Natl. Acad. Sci. U.S.A. **110:**18674-18679.
19. **Hirota SA, Iablokov V, Tulk SE, Schenck LP, Becker H, Nguyen J, Al Bashir S, Dingle TC, Laing A, Liu J, Li Y, Bolstad J, Mulvey GL, Armstrong GD, MacNaughton WK, Muruve DA, MacDonald JA, Beck PL.** 2012. Intrarectal instillation of *Clostridium difficile* toxin A triggers colonic inflammation and tissue damage: development of a novel and efficient mouse model of *Clostridium difficile* toxin exposure. Infect. Immun. 80(12):4474-84.
20. **Vohra P, Poxton IR.** 2012. Induction of cytokines in a macrophage cell line by proteins of *Clostridium difficile*. FEMS Immunol Med Microbiol. 65:96-104.
21. **Lyerly DM, Saum KE, MacDonald DK, Wilkins TD.** 1985. Effects of *Clostridium difficile* toxins given intragastrically to animals. Infect. Immun. **47:**349-352.
22. **Lima AA, Lyerly DM, Wilkins TD, Innes DJ, Guerrant RL.** 1988. Effects of *Clostridium difficile* toxins A and B in rabbit small and large intestine *in vivo* and on cultured cells *in vitro*. Infect. Immun. **56:**582-588.
23. **Sun X, Savidge T, Feng H.** 2010. The enterotoxicity of *Clostridium difficile* toxins. Toxins (Basel). **2:**1848-80.
24. **Savidge TC, Pan WH, Newman P, O'brien M, Anton PM, Pothoulakis C.** 2003. *Clostridium difficile* toxin B is an inflammatory enterotoxin in human intestine. Gastroenterology.**125:**413-420.
25. **Weiss K.** 2009. Toxin-binding treatment for *Clostridium difficile*: a review including reports of studies with tolevamer. Int. J. Antimicrob. Agents. **33:**4-7.
26. **Bauer MP, van Dissel JT.** 2009. Alternative strategies for *Clostridium difficile* infection. Int. J. Antimicrob. Agents. **33**(Suppl 1)**:**S51-56.
27. **Electronic Code of Federal Regulations**. 2010. 21 CFR §182.2729.
28. **Solomon K, Webb J, Ali N, Robins RA, Mahida YR.** 2005. Monocytes are highly sensitive to *Clostridium difficile* toxin A-induced apoptotic and nonapoptotic cell death. Infect. Immun. **73:**1625-1634.
29. **Fernando SA, Wilson GS.** 1992. Studies of the 'hook' effect in the one-step sandwich immunoassay. J. Immunol. Methods. **151:**47-66.
30. **Barker RH Jr, Dagher R, Davidson DM, Marquis JK.** 2006. Review article: tolevamer, a novel toxin-binding polymer: overview of preclinical pharmacology and physicochemical properties. Aliment. Pharmacol. Ther. **24:**1525-1534.
31. **Louie TJ, Peppe J, Watt CK, Johnson D, Mohammed R, Dow G, Weiss K, Simon S, John JF Jr, Garber G, Chasan-Taber S, Davidson DM; Tolevamer Study Investigator Group.** 2006. Tolevamer, a novel nonantibiotic polymer, compared with vancomycin in the treatment of mild to moderately severe *Clostridium difficile*-associated diarrhea. Clin. Infect. Dis. **43:**411-420.

32. **Hofmann F, Herrmann A, Habermann E, von Eichel-Streiber C.** 1995. Sequencing and analysis of the gene encoding the alpha-toxin of *Clostridium novyi* proves its homology to toxins A and B of *Clostridium difficile*. Mol. Gen. Genet. **247:**670-679.

33. **Demarest SJ, Salbato J, Elia M, Zhong J, Morrow T, Holland T, Kline K, Woodnutt G, Kimmel BE, Hansen G.** 2005. Structural characterization of the cell wall binding domains of *Clostridium difficile* toxins A and B; evidence that Ca2+ plays a role in toxin A cell surface association. J. Mol. Biol. **346:**1197-1206.

34. **Mitchell NJ, Kumi J, Aleser M, Elmore SE, Rychlik KA, Zychowski KE, Romoser AA, Phillips TD, Ankrah NA.** 2014. Short-term safety and efficacy of calcium montmorillonite clay (UPSN) in children. Am. J. Trop. Med. Hyg. **91:**777-85.

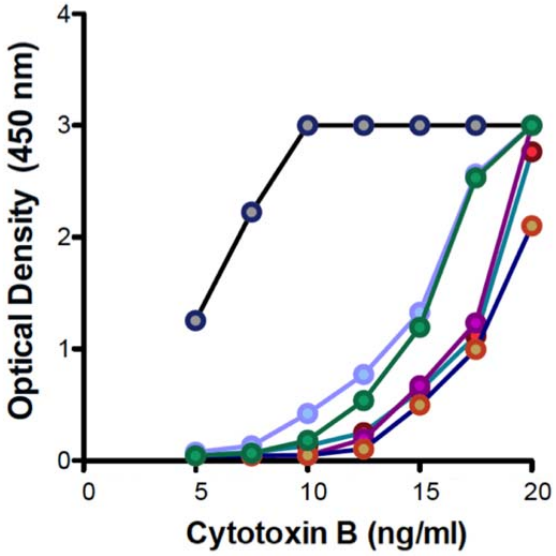

FIGURE 1. Untransformed EIA calibration curves. The mean optical density (*y*-axis) for each of six randomly selected cytotoxin B EIA calibration curves is plotted as a function of cytotoxin B concentration (*x*-axis). The data are expressed as means ± SEM.

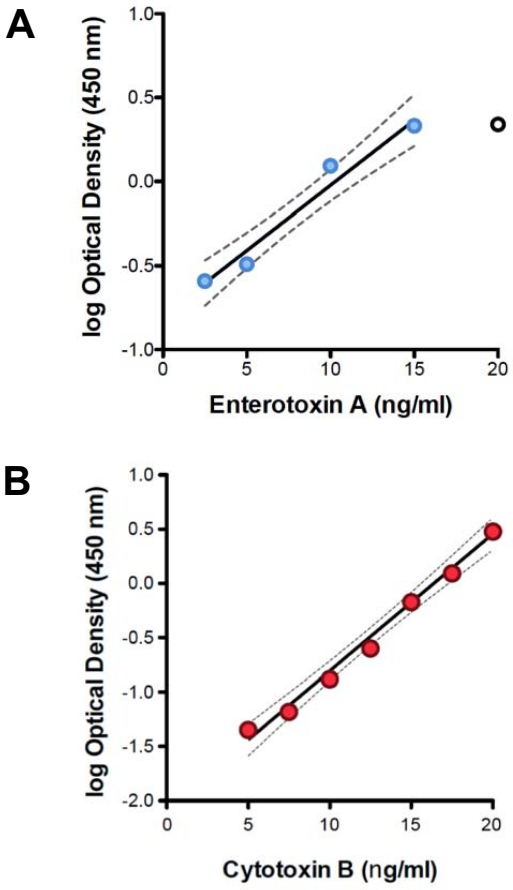

FIGURE 2. Linear regression of representative logarithm-transformed qEIA calibration data. The logarithm (base 10) of the optical density of each reference standard (*y-axis)* was determined by EIA and plotted against toxin concentration (*x*-axis). Circles denote median calibration data from *n* repeated replicates. The solid line denotes linear regression with 95% confidence limits, while dashed lines denote the boundaries of the calculated 95% confidence interval. **Panel A,** linear regression of enterotoxin A data ($n = 5$, $R^2 = 0.968$). **Panel B,** linear regression of cytotoxin B calibration data ($n = 4$, $R^2 = 0.966$).

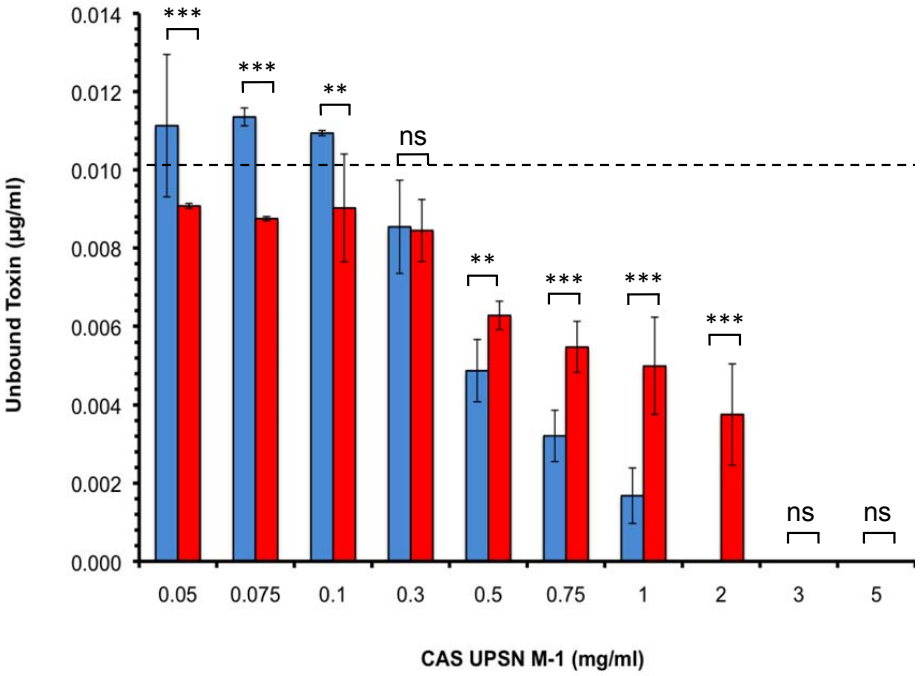

FIGURE 3. The selective and dose-dependent adsorption of *C. difficile* toxins by CAS UPSN M-1 *in vitro.* CAS UPSN M-1 was supplemented to a final concentration between 0.05 to 5 mg/ml (100-fold range) (*x*-axis), while toxin concentration was fixed to 10 µg/ml (dashed line). After a 10-min co-incubation, the mineral-toxin complexes were removed by centrifugation and the residual concentration of enterotoxin A (blue) and cytotoxin B (red) was determined by quantitative EIA (*y*-axis). The data are expressed as the means ± SD. The statistical significance of differences in toxin-specific binding-ability are reported for each concentration. Abbreviations: ns, statistically nonsignificant ($P > 0.05$); **, statistically significant ($P < 0.01$); ***, statistically significant ($P < 0.001$).

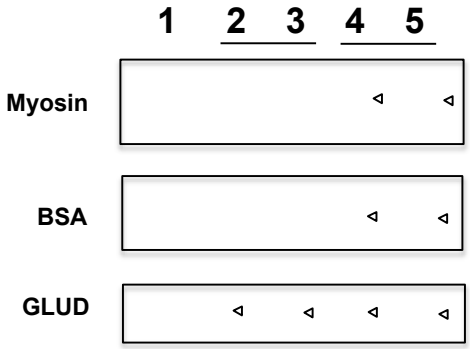

FIGURE 4. Non-therapeutic protein-binding assay. SDS-PAGE gels illustrating differential binding of myosin (top panel), bovine serum albumin (BSA) (middle panel), and glutamate dehydrogenase (GLUD) (bottom panel). Lane 1, untreated reference protein (negative control); Lanes 2-3, CAS UPSN M-1-treated protein samples (duplicates); Lanes 4-5, eluate of protein-bound-CAS UPSN M-1 complexes (duplicates). White carrots are used to mark lanes that are devoid of a protein band.